Cell Reports, Volume *30*

Supplemental Information

Chromatin Remodeling and Immediate Early Gene Activation by SLFN11 in Response to Replication Stress

Junko Murai, Hongliang Zhang, Lorinc Pongor, Sai-Wen Tang, Ukhyun Jo, Fumiya Moribe, Yixiao Ma, Masaru Tomita, and Yves Pommier

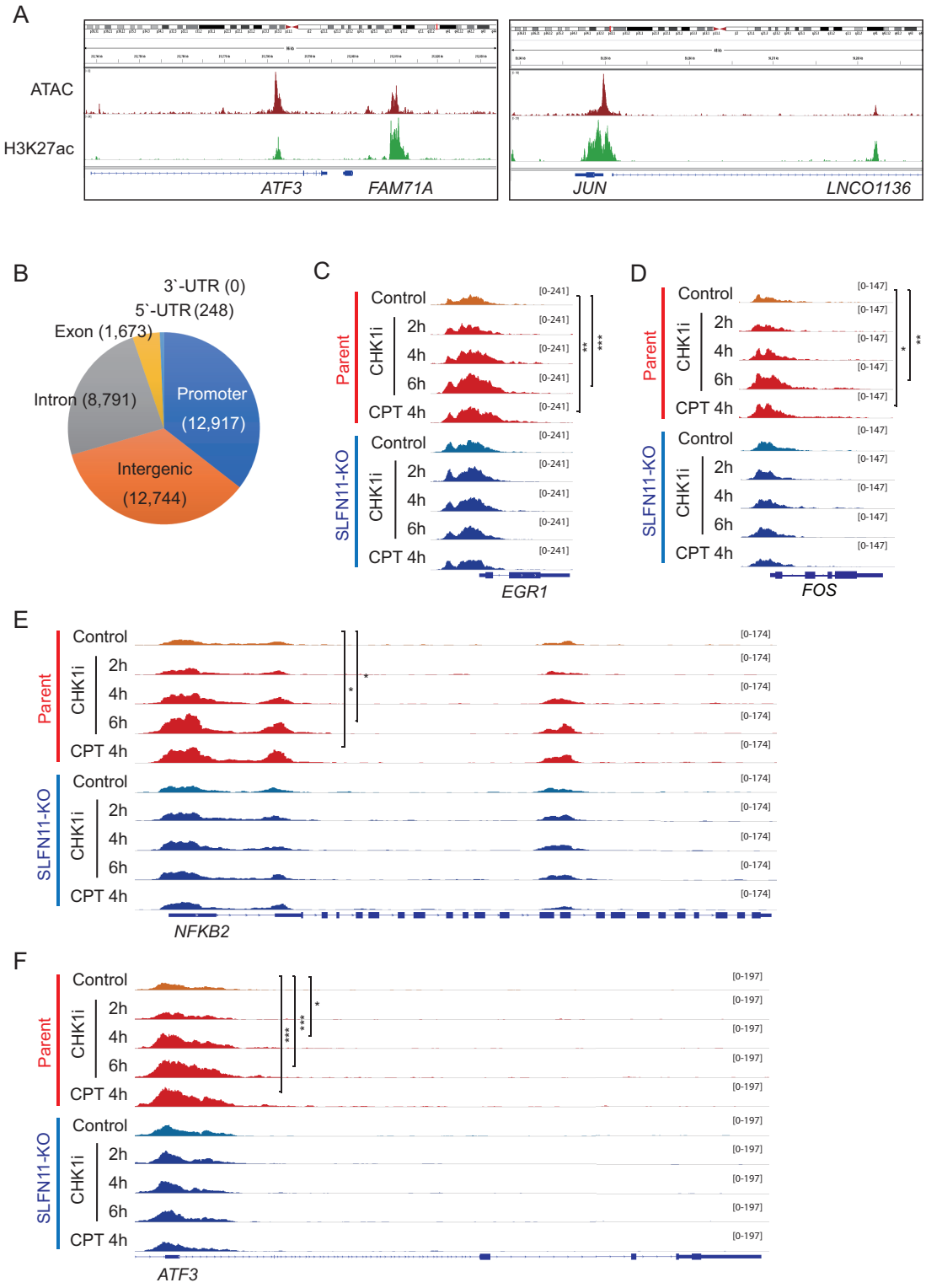

Figure S1. SLFN11 increases chromatin accessibility under CHK1i or CPT treatment, Related to Figure 1. (A) Representative IGV tracing for ATAC-Seq (red) and H3K27 acetylation Chip-Seq (green) under basal condition in CCRF-CEM parental cells. **(B)** A pie chart showing the fraction of genomic location of ATAC peaks under basal condition in CCRF-CEM parental cells. The number of peaks in each region is shown within parenthesis. **(C-F)** Representative IGV sequencing tracks for the indicated gene loci are shown. Signal in promoters of untreated and treated samples were compared using the Poisson test, which is similarly applied by MACS for peak calling (Zhang et al., 2008). *p ≤ 0.05, **p ≤ 0.01, ***p ≤ 0.001

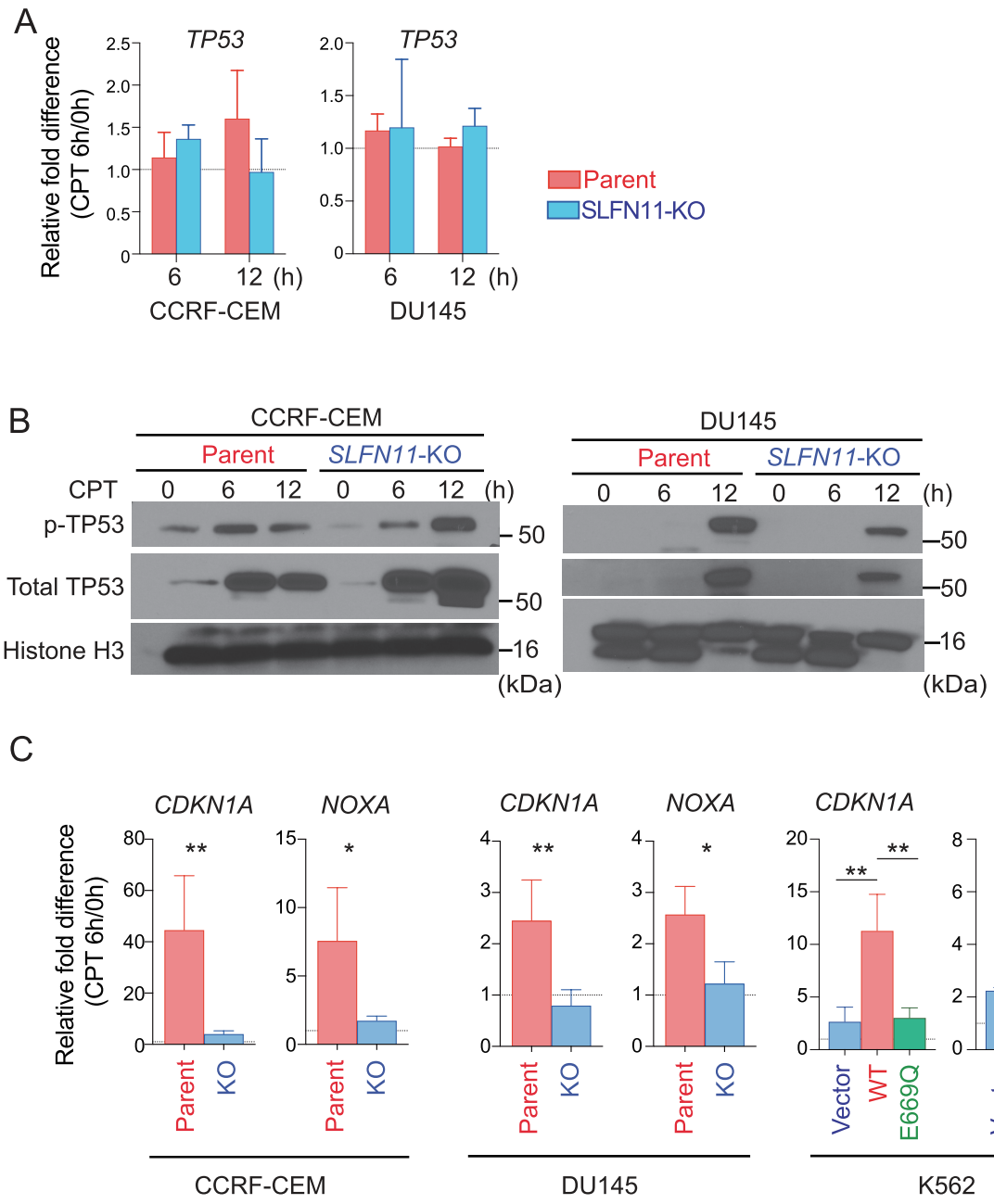

Figure S2. Transcription activation by SLFN11 is TP53-independent, Related to Figure 4

(A, C) Bar graphs of quantitative real-time reverse transcription PCR (qRT-PCR) for the indicated gene expression, for the indicated time and for the indicated treatment (100 nM CPT in CCRF-CEM and DU145, and 250 nM CPT in K562 cells). Each transcript was normalized with expression level of 18S RNA. Error bar represent standard deviations (SD, n=3). Results are representative of two independent experiments. *p ≤ 0.05, **p ≤ 0.01 **(B)** Western blot for the indicated antibodies under the indicated condition (100 nM CPT in CCRF-CEM and DU145, and 250 nM CPT in K562 cells) in the indicated cell lines.

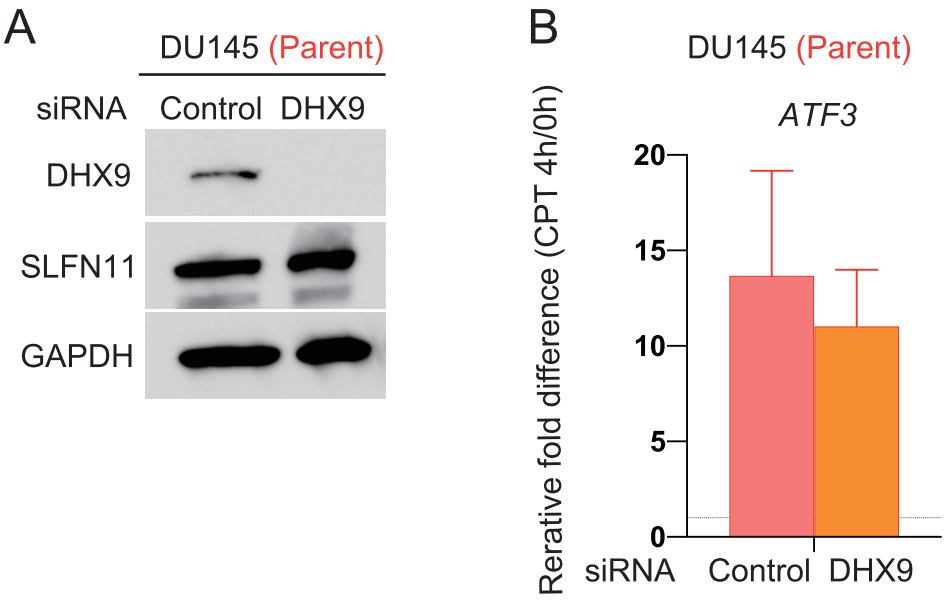

Figure S3. DHX9 has not impact on transcription activation by SLFN11, Related to Figure 4

(A-B) DU145 parental cells were transfected with siRNA for DHX9 or non-targeting control siRNA. (A) Western blot for the indicated antibodies. Two days after the transfection, cells were collected and lysed. (B) Bar graphs of qRT-PCR for *ATF3* expression in DU145 parental cells treated or non-treated by CPT (100 nM) for 4 hours. Cells were treated two days after the transfection.

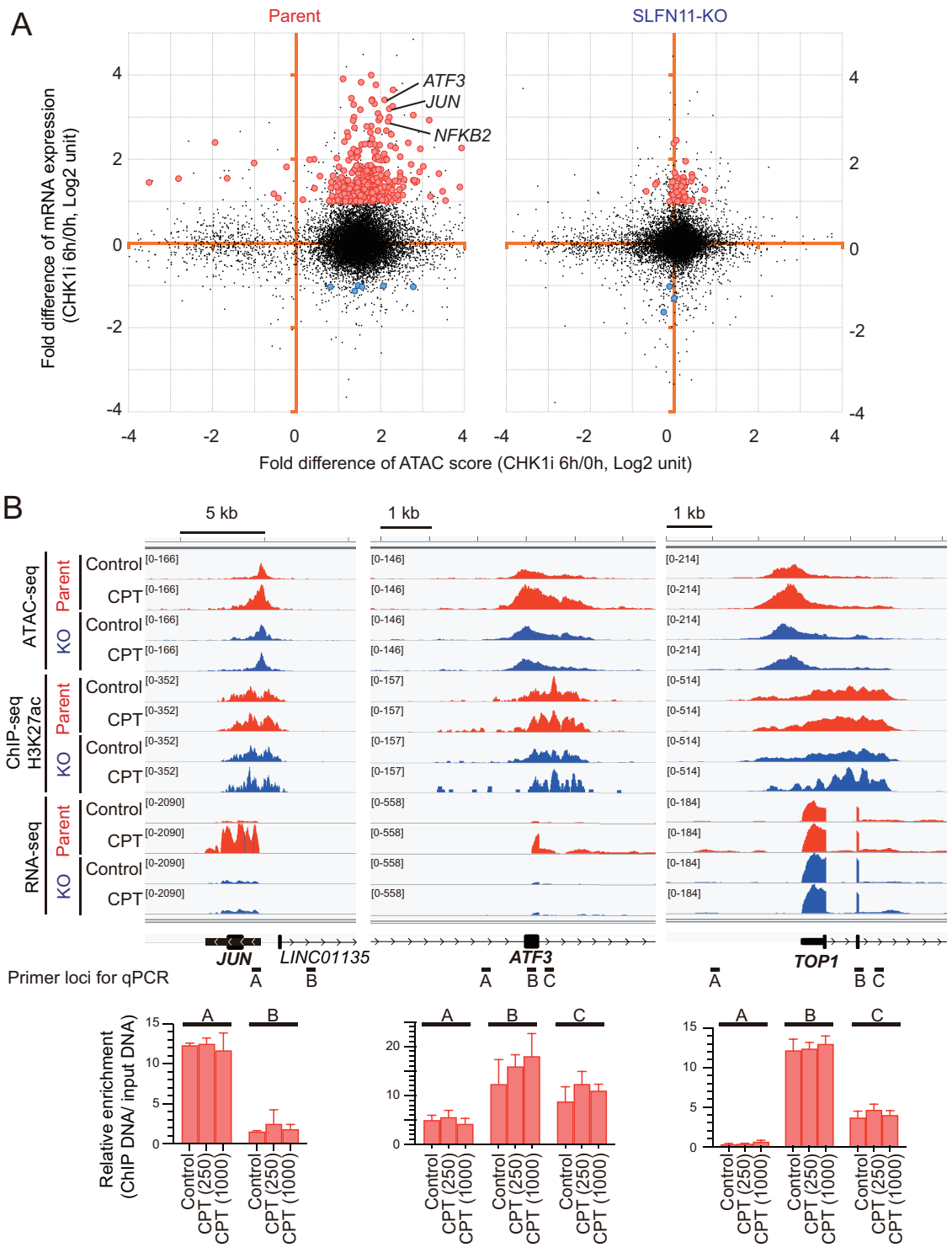

Figure S4. Chromatin accessibility occurs irrespectively of gene regulation and without global chage in H3K27ac level, Related to Figure 6

(A) The ATAC-seq data (Figure 1G) and the RNA-seq data (Figure 2A-B) were reanalyzed. Dot blots representing fold difference of mRNA expression (CHK1i 4h/0h) (y-axis) and fold difference of ATAC score (CHK1i 4h/0h) (x-axis) in CCRF-CEM parental (left) and SLFN11-KO cells (right). Some of representative immediate early genes are annotated. Upregulated (>2.0-fold and p<1E-07) and downregulated (<-2.0-fold and p<1E-07) genes are colored with red and blue, respectively.

(B) Representative sequencing tracks around the indicated gene loci for the indicated conditions in CCRF-CEM parent and SLFN11-KO (up). Enrichment of the active histone mark H3K27Ac around the indicated gene loci was examined by chromatin immunoprecipitation (ChIP) assay in CCRF-CEM parental cells with or without CPT treatment (250 nM or 1000 nM, 4h, bottom). The loci of primer sets for ChIP qPCR are shown at the bottom of each sequence track. Results are representative data of three independent experiments and the average of three technical repeats with ± SD.